

On Plastic Instability and Fracture in Upset-Forging

Yilong Bai

Institute of Mechanics, Chinese Academy of Sciences, Beijing,
People's Republic of China

and

Bradley Dodd

Department of Engineering, University of Reading, Whiteknights,
Reading RG6 2AY, Berkshire, Great Britain

(Received: 8 May 1984)

ABSTRACT

A shear instability criterion is described which is applied to the onset of surface cracking in the upset-forging of cylinders. In an element at the equatorial free surface there are three possible planes along which an instability can initiate, these are the planes of maximum shear stress. In the development of the criterion a characteristic material constant is derived which includes the material density and specific heat, as well as the current shear stress and the rate of thermal softening at instability.

The two conditions that must be fulfilled for the onset of this type of shear instability are described. It is shown that one of the modes of instability coincides with the experimentally observed linear fracture locus on the hoop strain-axial strain plane. Further, a second mode of instability is suppressed, and the third possible mode is shown to be metastable. It is shown that the observations concerning the three modes of shear instability are consistent with the observed fracture locus, crack orientations and strain perturbations prior to fracture.

NOTATION

θ, r, z	cylindrical co-ordinates
$\epsilon_{\theta}, \epsilon_z, \epsilon_r$	natural hoop, axial and radial strains at the equator, respectively

a	plane-strain fracture-strain
ρ	density
c_v	specific heat
τ	shear stress
p	rate of thermal softening, $-(\partial\tau/\partial T)_{\gamma,\dot{\gamma}}$
q	rate of strain hardening, $(\partial\tau/\partial\gamma)_{\dot{\gamma},T}$
$\gamma, \dot{\gamma}$	engineering shear strain and shear strain rate, respectively
$\bar{\sigma}$	effective stress
$\bar{\epsilon}$	effective strain
$d\epsilon$	plastic strain increment
$d\gamma$	plastic shear strain increment
A, K, n, m	constants
M	material constant
α	strain increment ratio $d\epsilon_\theta/d\epsilon_z$
W_p	plastic work per unit volume
f, G	functions of α
T	temperature

Subscripts

f fracture

i instability

k modes I, II or III

s pure shear

INTRODUCTION

Upsetting

Upsetting is the axial compression of the whole or part of the length of a workpiece. Often, the compression of part of the length of a workpiece is called heading. The process of upsetting is one of the simplest forging operations and is common in industry.

Axial compression of cylinders is a test which is used to obtain the compressive stress-strain behaviour of materials. In compression testing care must be taken to ensure good lubrication between the platens and the workpiece, otherwise barrelling will occur. Any barrelling results in induced hoop tensile strains at the surface of the

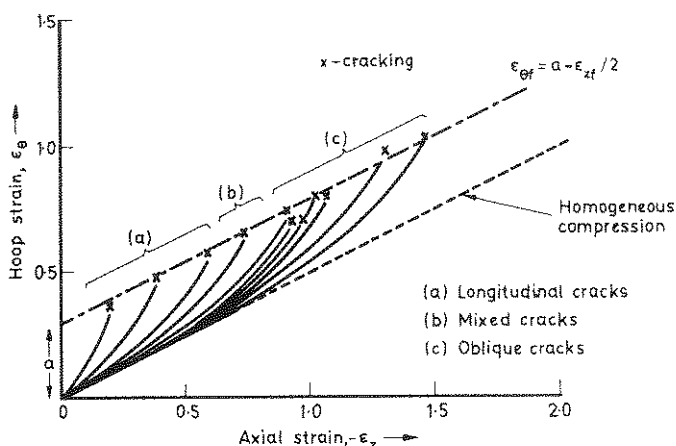


Fig. 1. Straight-line fracture condition observed by Kudo and Aoi.¹

workpiece. If barrelling is extensive, then these induced strains can lead to premature fracture.

Kudo and Aoi¹ controlled the degree of barrelling in their tests by using different die sets, lubricants and specimen aspect ratios (height-diameter ratios). For a 0.45% carbon steel they measured the strain histories to fracture at the equators of a series of cylindrical specimens, see Fig. 1. They found that the locus of fracture strains is linear with a slope of $-\frac{1}{2}$ and can be described simply by the equation

$$\epsilon_{\theta f} = a - \epsilon_{zf}/2 \quad (1)$$

where $\epsilon_{\theta f}$ is the hoop fracture strain, ϵ_{zf} is the axial fracture strain and a is the plane-strain fracture-strain.

The application of the upsetting process to studies of free surface ductility and theories of ductile fracture has been described in detail by Jenner and Dodd.²

Plastic instability

Localization of plastic deformation is a prerequisite for ductile fracture.³ This localization is referred to as plastic instability. Two classes of plastic instability are of importance in the plastic deformation of metals, viz. tensile and shear instabilities.

The most common example of a tensile instability is necking that occurs in a tensile test on, for example, a cylindrical rod specimen. Tensile instability occurs at the maximum load after which plastic deformation is confined to the neck. As deformation proceeds the cross-section of the centre of the neck becomes smaller until, ultimately, fracture occurs. However, even in this case final separation of the specimen results from localized deformation along shear bands.⁴

The best example of a shear instability occurs in torsion testing of thin-walled tubular specimens. In this case the onset of instability coincides with a maximum in the flow stress.⁵ Before this maximum is reached the whole gauge length deforms uniformly, whereas after the maximum deformation is confined to a small number of shear bands along which, eventually, fracture occurs.

Localized shear band formation has been observed in ordnance testing, high-speed forming and cryogenic deformation.⁶⁻⁸ In all of these cases the heat generated by the plastic deformation is appreciable. When the heat generated is high it is possible that adiabatic conditions will be approached. For adiabatic deformation, the applied strain rates are so high that the heat generated does not have time to be conducted away from the deforming region. This leads to thermal softening of the plastic region, which promotes greater localization of deformation. Ultimately, under these circumstances, failure will occur by catastrophic shear in very narrow bands. Although adiabatic plastic deformation is thermodynamically possible, practically there will always be some heat conducted away from the deforming region.

A THERMOPLASTIC SHEAR INSTABILITY CRITERION

Rogers⁸ noted that in processes such as forging, interface friction between the dies and workpiece causes the plastic deformation to be inhomogeneous and to localize. In such regions of localization the temperature rise resulting from the plastic work can be high. These localized regions consist predominantly of shear deformation.

Based on adiabatic considerations, Culver⁹ developed an adiabatic shear instability criterion which he applied successfully to torsion tests. It can be shown analytically¹⁰ and also by dimensional analysis¹¹ that this criterion is applicable to non-adiabatic conditions. For most

metals the criterion can be written simply as

$$\frac{K\tau p}{\rho c_v q} = 1 \quad (2)$$

where K is the fraction of the plastic work converted into heat, τ is the shear stress at instability, p is the rate of thermal softening, $p = -(\partial\tau/\partial T)_{\dot{\gamma}, \dot{\gamma}}$, ρ is the material density, c_v is the specific heat of the material and q is the rate of strain hardening, $q = (\partial\tau/\partial\gamma)_{\dot{\gamma}, T}$. Kudo and Tsubouchi¹² also discussed strain concentration in torsion due to temperature rise.

The concept of thermoplastic shear instability possesses wider generality since, first, adiabatic deformation is never attained practically and, second, in forging and related compressive processes the temperature increase due to the inhomogeneous deformation may be appreciable. In addition, under adiabatic conditions the shear bands are very narrow, but as the deformation becomes more non-adiabatic the shear bands become broader, in the extreme case the width of the shear band tends to infinity; that is, there is no shear localization.

In the following sections the thermoplastic shear instability criterion is used to explain the onset of instability and fracture at the free surface in upsetting. The criterion is equally applicable to the onset of edge cracking in rolling of flat plates, since these cracks have the same origin as those that occur in upsetting.¹³

APPLICATION OF THERMOPLASTIC SHEAR INSTABILITY TO UPSET-FORGING

To use the criterion for upsetting, it is necessary to consider shear deformation on an infinitesimally small cubical element at the equatorial free surface of a cylinder. The criterion was obtained analytically for the simple shear state¹⁰ and critical shear strains were found experimentally from torsion tests.⁹ In the case of a torsion test, the maximum shear strain rate is fixed on a material section during the course of plastic deformation. Hence, the measured critical shear strain is a material parameter.

The circumstances in upsetting are a little different. The equatorial free surface element is subjected to a combined stress state (which is neither simple shear nor plane-strain). Observations show, however,

that the crack orientations have a close connection with the bands of shear localization on the maximum shear planes. It is therefore assumed here that an element at the equatorial free surface of a cylinder can develop a localized shear band only when the following two conditions are fulfilled: (1) a certain shear instability condition must be satisfied within the element and (2) at that moment there is no normal strain increment, i.e. $d\varepsilon_\gamma = 0$ on the maximum shear plane under consideration. The second condition is equivalent to $d\varepsilon_\theta = 0$, $d\varepsilon_r = 0$ or $d\varepsilon_z = 0$, respectively, due to constant volume in the plastic regime, provided θ , r and z are principal axes. For an element at the equatorial free surface in an isotropic material they are principal axes due to symmetry. Accordingly, the maximum shear plane is subjected instantaneously to similar conditions as the maximum shear plane in simple shear. So it is reasonable to adopt eqn. (2) as the aforementioned shear instability in simple shear.

Because the shear instability criterion in eqn. (2) only contains instantaneous parameters and has no explicit connection with history effects, it can be assumed that at the onset of instability on a shear plane the parameters τ_i , q_i and p_i satisfy the criterion. When p_i is assumed to be constant,

$$\frac{\tau_i}{q_i} = \frac{\rho c_v}{K p_i} = M \quad (3)$$

where M is a characteristic material constant. In torsion, M can be expressed by $M = \gamma_i/n$, where γ_i is the critical shear strain and n the strain hardening exponent, if the stress-strain relation is $\tau = A_1 \gamma^n$. The three planes upon which shear instability may develop are: (i) the plane oriented at 45° to the θ -axis and 45° to the r -axis (mode I); (ii) the plane oriented at 45° to the θ -axis and 45° to the z -axis (mode II); and (iii) the plane oriented at 45° to the z -axis and 45° to the r -axis (mode III). Which one of these three planes will undergo instability will depend on the stress and strain history.

To calculate the values of τ_i/q_i on the three possible planes, the following assumptions are made:

- (i) the material strain hardens isotropically,
- (ii) the isothermal strain rate-constant stress-strain relationship is of the power law form $\bar{\sigma} = A_2 \bar{\varepsilon}^n$, where $\bar{\sigma}$ and $\bar{\varepsilon}$ are the effective stress and strain, respectively and
- (iii) the von Mises yield function equals the plastic potential.

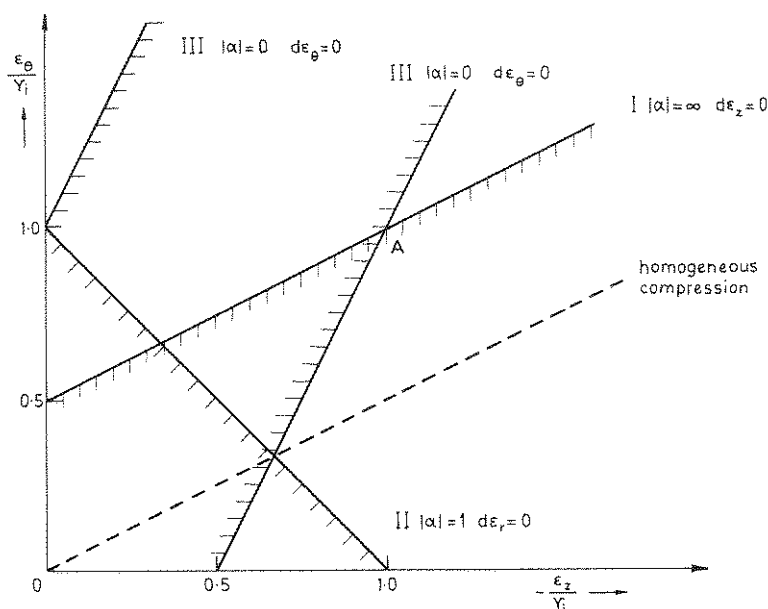


Fig. 2. The three modes of instability with the required strain path slopes.

From condition (1) and eqn. (3) it is possible (see the next section) to represent the three instability conditions on the $(\varepsilon_\theta - \varepsilon_z)$ plane as in Fig. 2. The formulae for these cases are

$$\begin{aligned} \varepsilon_\theta &= \frac{\gamma_i}{2} - \frac{\varepsilon_z}{2} && \text{for mode I} \\ \varepsilon_\theta &= \gamma_i + \varepsilon_z && \text{for mode II} \\ \varepsilon_\theta &= \gamma_i \pm 2\varepsilon_z && \text{for mode III} \end{aligned} \quad (4)$$

where, as mentioned above,

$$\gamma_i = nM \quad (5)$$

INTERPRETATION OF THE THREE POSSIBLE INSTABILITY MODES

In this section, conditions (1) and (2) are examined in detail in order to reach an understanding of the differences between the three shear instability modes mentioned above.

It has been shown by Kudo and Aoi,¹ and subsequently by others, that all the equatorial strain paths in upsetting of cylinders can be described by

$$\frac{d^2 \varepsilon_\theta}{d|\varepsilon_z|^2} \geq 0 \quad (6)$$

and

$$\left. \frac{d\varepsilon_\theta}{d|\varepsilon_z|} \right|_{\varepsilon_r \rightarrow 0} \geq \frac{1}{2} \quad (7)$$

with $|d\varepsilon_\theta/d\varepsilon_z|$ increasing with reduction in height. It is instructive to interpret the three possible instability modes in relation to these experimental results.

Using the three assumptions given in the previous section it is possible to derive an equation for the Lagrangian multiplier in the Lévy-Mises equations in terms of a function of the plastic work, W_p , see the Appendix for the method of derivation. By means of this function, together with the three expressions for the plastic work increment corresponding to the three maximum shear planes and also taking into account the general case of non-linear strain paths, it can be shown that the rate of strain hardening on each of the three possible planes is given by

$$q_k = \frac{m W_p^{m-1}}{4A[1 + f_k(\alpha)(d\varepsilon_{\gamma k}/d\gamma_k)]} \quad (8)$$

where

$$f_k(\alpha) = \left\{ \begin{array}{ll} \frac{-3\alpha}{(2\alpha+1)} & \text{for mode I} \\ \frac{-3(\alpha+1)}{2(\alpha-1)} & \text{for mode II} \\ \frac{3}{(\alpha+2)} & \text{for mode III} \end{array} \right\} \quad (9)$$

Also,

$$\frac{d\varepsilon_{\gamma k}}{d\gamma_k} = \left\{ \begin{array}{ll} \frac{1}{(2\alpha+1)} & \text{for mode I} \\ \frac{(1+\alpha)}{(1-\alpha)} & \text{for mode II} \\ \frac{\alpha}{(\alpha+2)} & \text{for mode III} \end{array} \right\} \quad (10)$$

$m = 2n/(n+1)$ and $A = 3/[2A_2^{2/(n+1)}(n+1)^{2n/(n+1)}]$.

Notice that here the maximum shear strain increments are physically meaningful and expressed as

$$\left. \begin{aligned} d\gamma_I &= |d\varepsilon_\theta - d\varepsilon_r| \\ d\gamma_{II} &= |d\varepsilon_\theta - d\varepsilon_z| \\ d\gamma_{III} &= |d\varepsilon_r - d\varepsilon_z| \end{aligned} \right\} \quad (11)$$

Using the same procedure as in the derivation of eqns. (8) it can be shown that the shear stress on each maximum shear plane is given by

$$\tau_k^2 = \frac{W_p^m}{2A} G_k(\alpha) \quad (12)$$

where

$$G_k(\alpha) = \left\{ \begin{array}{ll} \frac{(2\alpha + 1)^2}{4(\alpha^2 + \alpha + 1)} & \text{for mode I} \\ \frac{(\alpha - 1)^2}{4(\alpha^2 + \alpha + 1)} & \text{for mode II} \\ \frac{(\alpha + 2)^2}{4(\alpha^2 + \alpha + 1)} & \text{for mode III} \end{array} \right\} \quad (13)$$

The plastic shear strain increments are

$$d\gamma_k = \sqrt{2AG_k(\alpha)} W_p^{-m/2} dW_p = \frac{\sqrt{2AG_k(\alpha)}}{1 - m/2} dW_p^{1-m/2} \quad (14)$$

From eqns. (12) and (14) it can be seen that the shear stress and the corresponding strain increments are both given in terms of functions of the plastic work and functions of the instantaneous slope of the strain path, $G_k(\alpha)$. Functions $G_k(\alpha)$ only contain the instantaneous strain path slopes; the stress and strain histories are reflected solely in the plastic work functions.

According to the discussion in the last section at the onset of thermoplastic shear instability two conditions must be fulfilled:

$$\frac{\tau_{ki}}{q_{ki}} \geq M \quad (15)$$

and

$$d\varepsilon_{\gamma_{ki}} = 0 \quad (16)$$

It follows from eqn. (16) that the corresponding values for α for the onset of instability are

$$\alpha = \left. \begin{array}{ll} -\infty & \text{for mode I} \\ -1 & \text{for mode II} \\ 0 & \text{for mode III} \end{array} \right\} \quad (17)$$

For these values of α , $f_k(\alpha_i) < \infty$ and $G_k(\alpha_i) = G_{\max} = 1$.

With $G_k(\alpha) = 1$ at instability, the criterion given by eqn. (15) becomes

$$\frac{\tau_i}{q_i} = 2 \frac{\sqrt{2A}}{m} W_{pi}^{1-m/2} \geq M \quad (18)$$

To obtain a more convenient criterion for each mode it is necessary to carry out a path-dependent integration. This is rather difficult to do without making simplifying assumptions concerning the strain paths, such as linear straining. However, it is still possible to obtain a physical understanding of a stable deformation condition. From eqns. (14) and (18), the criterion can be expressed in the form

$$\int_0^{\gamma_{ki}} \frac{d\gamma_k}{\sqrt{G_k(\alpha)}} < nM \quad (19)$$

where γ_{ki} is only the upper limit of the integral. Because $G_{k \max} = 1$, and using eqns. (11), condition (19) reduces to

$$\int_0^{\gamma_{ki}} d\gamma_k = \gamma_{ki} \leq \int_0^{\gamma_{ki}} \frac{d\gamma_k}{\sqrt{G_k(\alpha)}} < nM \quad (20)$$

which provides a threshold to the instability phenomena; tests with any permissible loading paths in upsetting cannot cross the threshold line without the onset of instability leading to ductile fracture. Now it is necessary to discuss the nature of γ_{ki} in eqn. (20). γ_k is the integration of the maximum shear strain increment $d\gamma_k$. Because of the definition of $d\gamma_k$, eqn. (11), and because the maximum shear strains are not fixed on a material section in upsetting, γ_k are not, in general, the maximum shear strains on the corresponding planes. Hence, γ_k are just the integration of the differences between the principal strain increments which are greater than any instantaneous maximum shear strains, because the maximum shear strain planes rotate and the values of γ_k are the accumulation of all the instantane-

ous maximum shear strain increments. From eqns. (11) and (20) the straight-line relationships between ε_0 and ε_z given by eqn. (4) define the threshold which denotes an upper bound to stable deformation.

It is natural at this stage to raise the following questions. (i) Why is it that it is only the mode I instability threshold which coincides with the experimentally determined fracture locus? (ii) Why is it that mode III instability is always suppressed? (iii) Why is it that mode II instability is activated on the threshold of mode I, and not on its own threshold?

In order to answer these questions it is necessary to examine the second condition for the onset of shear instability in more detail.

Simply, the slopes of the strain paths necessary for each mode of instability due to condition (2) are: mode I, $\alpha = -\infty$; mode II, $\alpha = -1$ and mode III, $\alpha = 0$. From strain paths determined experimentally, or eqns. (6) or (7), it is clear that α can never equal zero. Therefore, mode III instability is suppressed.

The behaviour of function G will now be explored. The physical implication of the second condition for the onset of shear instability can be observed through functions $G_k(\alpha)$. $G_{k \max} = 1$ corresponds to condition (2) and implies a state for which the amount of shear deformation can be achieved with the minimum plastic work, see eqn. (14).

Figure 3 shows the variation of function $G_k(\alpha)$ with $1/\alpha$. It can be seen that $G_k(\alpha)$ is always within the range

$$0 \leq G_k(\alpha) \leq 1 \quad (21)$$

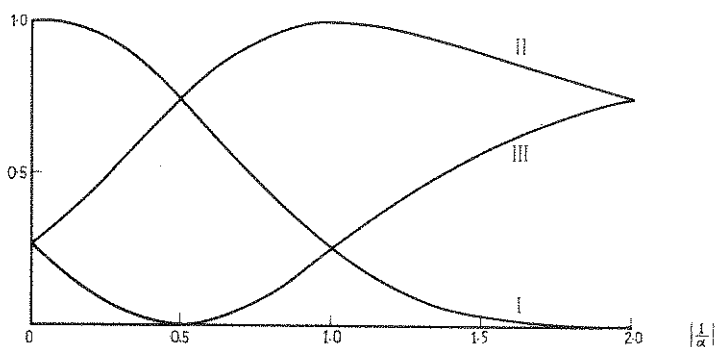


Fig. 3. The relationship between functions $G_k(\alpha)$, ordinate, and $1/\alpha$.

When $G_k(\alpha) = 0$, then there can be no increment of shear deformation on the corresponding shear plane. On the other hand, a maximum in G_k leads to the largest $d\gamma_k$. Importantly, only maximum values of $G_k(\alpha)$ are observed for modes I and II at $\alpha = -\infty$ and -1 , respectively. Also

$$\begin{aligned} G_{I \max} > G_{II} \quad \text{and} \quad G_{III} \quad \text{at} \quad \alpha = -\infty \\ G_{II \max} > G_I \quad \text{and} \quad G_{III} \quad \text{at} \quad \alpha = -1 \end{aligned} \quad (22)$$

From experimental observations it has been noted that $|\alpha| > \frac{1}{2}$; indeed, the value of $|\alpha|$ increases along a straining path to high values. From Fig. 3 it can be seen that in the case of mode I instability $G_I(\alpha)$ increases with increasing $|\alpha|$ steadily until $|\alpha| = \infty$. Therefore, at $|\alpha| = \infty$ with $G_I(\alpha) = 1$, mode I instability must be initiated eventually.

For mode II instability conditions are different. Figure 3 shows that $G_{II}(\alpha)$ reaches a maximum at $\alpha = -1$. For $\alpha < -1$, $G_{II}(\alpha)$ decreases with further reduction in height. This means that the element being considered can return to a stable state, $G_{II}(\alpha) < 1$, provided that shear instability does not occur at $\alpha = -1$ due to either the absence of a trigger or the non-fulfilment of condition (1). This is very different from the mode I case, in which $G_I = 1$ at $\alpha = -\infty$ is the final state. Once the element enters this state it can never leave, and therefore instability must occur eventually. Thus, in comparison with the mode I case, mode II instability is metastable. Of course, this does not exclude the reappearance of the condition $\alpha = -1$ and the possible initiation of mode II instability. In fact, this does happen after mode I instability.¹⁴

The experimental results obtained by Lee¹⁴ are of importance in relation to the foregoing discussion of the thermoplastic shear instability criterion. Using fine grids on cylinders, Lee observed a perturbation in the axial strain, ϵ_z , just before fracture. This perturbation is equivalent to $d\epsilon_z = 0$, and in the context of the above discussion means the onset of the mode I shear instability. After the perturbation in ϵ_z , Lee observed a region for which $d\epsilon_r = 0$; this is equivalent to the onset of mode II instability. Thus, it appears from Lee's experimental evidence that the onset of mode I instability triggers the onset of the subsequent mode II instability. Another feature is that mode II instability could only appear below the straight line $\alpha = -1$

in Fig. 2, owing to eqns. (6) and (7) and the behaviour of G . Therefore mode II instability can just be triggered beyond point A in Fig. 2, which corresponds to $\epsilon_\theta = -\epsilon_z = 2a$. Referring to Fig. 1 this point coincides rather accurately with the point at which mixed cracks appear in tests. Hence, the shear instability theory together with the important experimental evidence described by Lee are a possible explanation of the mode I and II macroscopic fractures which cannot be explained with either the maximum shear stress or maximum tensile stress theories.

APPENDIX

It is assumed that the yield function is always equal to a function of the plastic work:

$$f(\sigma_{ij}) - k(W_p) = 0 \quad (\text{A1})$$

Further, it is assumed that $f(\sigma_{ij})$ is the von Mises yield function

$$f(\sigma_{ij}) = J_2^{1/2} \quad (\text{A2})$$

where J_2 is the second invariant of the stress deviator tensor.

The uniaxial tensile test is used to determine k in eqn. (A1) and $d\lambda$ in the Lévy-Mises equations. It follows that

$$k = f = \sigma/\sqrt{3} \quad \text{and} \quad d\lambda = \frac{3}{2} \frac{dW_p}{\sigma^2} \quad (\text{A3})$$

where $dW_p = \sigma d\epsilon$. If power-law strain hardening in simple tension is assumed,

$$\sigma = A_2 \epsilon^n \quad (\text{A4})$$

then

$$d\lambda = \frac{A dW_p}{W_p^m} \quad (\text{A5})$$

where

$$m = 2n/(n+1) \quad \text{and} \quad A = 3/2(n+1)^{2n/(n+1)} A_2^{2/(n+1)} \quad (\text{A6})$$

Turning attention to simple shear,

$$dW_p = \tau d\gamma \quad (\text{A7})$$

and

$$d\gamma = 2d\lambda\tau = \frac{2A}{W_p^m} \tau dW_p \quad (\text{A8})$$

then

$$\left(\frac{\partial\tau}{\partial\gamma}\right) = \frac{mW_p^{m-1}}{4A} \quad \text{and} \quad W_p^{-m/2} dW_p = \frac{1}{\sqrt{2A}} d\gamma \quad (\text{A9})$$

and

$$\frac{\tau}{(\partial\tau/\partial\gamma)} = \left(\frac{2-m}{m}\right) \int_0^{\gamma_i} d\gamma = \left(\frac{2-m}{m}\right) \gamma_i \quad (\text{A10})$$

Considering an element at the equatorial free surface of a cylinder and confining attention to mode I, then

$$dW_p = \sigma_\theta d\varepsilon_\theta + \sigma_z d\varepsilon_z$$

Now

$$\tau = \frac{1}{2}(\sigma_\theta - \sigma_r) \quad \text{and} \quad d\gamma = d\varepsilon_\theta - d\varepsilon_r \\ p = \frac{1}{3}(\sigma_\theta + \sigma_r + \sigma_z)$$

therefore

$$dW_p = \tau d\gamma + 3(p - \tau) d\varepsilon_z \quad (\text{A11})$$

It follows that

$$d\gamma = \frac{2A}{W_p^m} [\tau^2 d\gamma + 3\tau(p - \tau) d\varepsilon_z] \quad (\text{A12})$$

From the above equations, it is possible to derive eqns. (8)–(12).

REFERENCES

1. Kudo, H. and Aoi, K., *J. Jpn. Soc. Tech. Plasticity*, **8** (1967) 17.
2. Jenner, A. and Dodd, B., Upsetting as a free surface ductility test, *4th Int. Conf. Prod. Engrs.*, Tokyo, August 1980.
3. Rogers, H. C., in *Fundamentals of deformation processing*, 9th Sagamore Army Materials Conf., Syracuse University Press, Syracuse, NY, 1964, p. 199.
4. Rogers, H. C., in *Ductility*, A.S.M., Metals Park, Ohio, 1967, p. 31.
5. Spretnak, J. W., U.S.A.F. Report AFML-TR-74-160, 1974.
6. Bedford, A. J., Wingrove, A. L. and Thompson, K. R. L., *J. Aust. Inst. Metals*, **19**(1) (1974) 61.

7. Rogers, H. C., *Adiabatic shearing—a review*, Drexel Univ. 1974.
8. Rogers, H. C., *A. Rev. Mater. Sci.*, **9** (1979) 283.
9. Culver, R. S., in (Rohde, R. W., Butcher, B. M., Holland J. R. and Karnes, C. H., Eds.), *Metallurgical Effects at High Strain Rates*, Plenum Press, New York, 1973, p. 519.
10. Bai, Y. L., A criterion for thermo-plastic shear instability, *Int. Conf. on the Metallurgical Effects of High Strain Rate Deformation and Fabrication*, Albuquerque, 1980.
11. Jenner, A., Bai, Y. L. and Dodd, B., *J. Strain Analysis*, **16** (3) (1981) 159.
12. Kudo, H. and Tsubouchi, M., *Ann. C.I.R.P.*, **19** (1971) 225.
13. Dodd, B. and Boddington, P., *J. Mech. Working Technol.*, **3** (1980) 239.
14. Lee, P. W., Ph.D. Thesis, Drexel University, 1972.